Supporting Information for

CuO-multimetal ferrites for synergically boosting peroxydisulfate activation and decontamination by adsorption and oxidation mechanisms

Zeynab Fadaei[1,2], Nadali Alavi[1,2,*], Babak Kakavandi[3,*], Abbas Shahsavani[1,2], Mohsen Sadani[1,2], Yueping Bao[4,*], Rasool Pelalak[5,6,*]

[1] Environmental and Occupational Hazards Control Research Center, Shahid Beheshti University of Medical Sciences, Tehran, Iran

[2] Department of Environmental Health Engineering, School of Public Health and Safety, Shahid Beheshti University of Medical Sciences, Tehran, Iran

[3] Department of Environmental Health Engineering, Alborz University of Medical Sciences, Karaj, Iran

[4] MOE Key Laboratory of Pollution Processes and Environmental Criteria, College of Environmental Science and Engineering, Nankai University, 300350 Tianjin, China

[5] Institute of Research and Development, Duy Tan University, Da Nang, Vietnam

[6] School of Engineering & Technology, Duy Tan University, Da Nang, Vietnam.

*** Corresponding authors:**

Environmental and Occupational Hazards Control Research Center, Shahid Beheshti University of Medical Sciences, Tehran, Iran. alavi@sbmu.ac.ir (N. Alavi)

Department of Environmental Health Engineering, Alborz University of Medical Sciences, Karaj, Iran. kakavandibvch@gmail.com (B. Kakavandi).

College of Environmental Science and Engineering, Nankai University, 300350 Tianjin, China. yueping.bao@nankai.edu.cn (Y. Bao).

Institute of Research and Development, Duy Tan University, Da Nang, Vietnam. rasoolpelalak@duytan.edu.vn (R. Pelalak).

Text S1

Copper nitrate ($Cu(NO_3)_2 \cdot 3H_2O$), ferric chloride hexahydrate ($FeCl_3.6H_2O$), copper chloride hydrate ($CuCl_2.2H_2O$), magnesium chloride ($MgCl_2 \cdot 6H_2O$), sodium hydroxide (NaOH, 99%), potassium persulfate (PS, $K_2S_2O_8$), ethanol (EtOH, C_2H_5OH), acetonitrile, acetic acid, tert-butyl alcohol (TBA, $C_4H_{10}O$), furfuryl alcohol (FFA), sodium azide (SA, NaN_3), and sodium hydroxide (NaOH) were analytical grade, obtained from Sigma Aldrich, and used as received, without further purification. Deionized (DI) water was used throughout the experiments.

Text S2

X-ray diffraction (XRD) was used to analyze the crystalline phase of all the all-prepared materials by using XRD Philips PW1730 PANalytical XPert Pro MPD, with Cu Kα radiation at a wavelength (λ = 1.5406 Å) with 2Θ range of 10 ◦ -80 ◦ . Field-emission scanning electron microscopy (SEM-EDS/JSM-6700F) equipped X-ray energy spectrum (EDS SAMX, SAMX, France) was used to characterize the external morphology and chemical elemental composition of as-synthesized catalysts. Meanwhile, an Energy-Dispersive X-ray (EDAX mapping was applied during FESEM analysis to evaluate the distribution of chemical elements. The nanostructure features of CuO and MMF nanoparticles in the MMF composite were investigated by using transmission electron microscopy (TEM, JEM-2100; Jeol; Japan). A Multi-point Brunner-Emmett-Teller analysis (ASAP; Micromeritics, USA) was used to determine the specific surface area and pore size of the synthesized MMF composite via the N_2 adsorption-desorption isotherms collected with a Micromeritics ASAP 2020 system. The magnetic measurements were performed on a Vibrating Sample Magnetometer (VSM)

(Lakeshore 7304, USA) for MMF and MMFC catalysts. To explore the change in surface charge, the zeta potentials of the as-prepared catalyst were measured using a Zetasizer Nano ZS90 (UK) in the range of pH values 1.0-11.0.

Text S3

Identification of the intermediary by-products was performed using a gas chromatograph coupled to a mass spectrometer (GC-MS-QP2010, SHIMADZU, Japan) using an NST 05 MS column (30 m x 0.25 mm x 0.25 μm coating thickness) composed of 95% dimethyl polysiloxane and 5% diphenyl. Initially, an extraction procedure based on 3 x 20 mL of CH2Cl2 was carried out in 40 mL of the CIP samples. In sequence, the combined organic layer was dried with anhydrous MgSO4 and concentrated by Nitrogen gas at 25°C. The oven initial temperature was 55°C, which was kept constant for 3 min, followed by an increase of 25°C min-1 until 300°C, then held for 6 min. The temperature of the injector and detector was 260°C, with an interface temperature of 240°C. The temperature of the ionization source was held at 250°C for the selection and quantification of the organic compounds. The equipment was adjusted to a voltage of 0.88 kV, generating an impact ionization of 70 eV for molecular fragmentation and production of ions in a mass/electric charge (m/z) field of 20 to 600 in order to identify the structure and determine the concentrations of the by-products in the samples. The structural configuration of the by-products is based on the NIST 08 library of the GC-MS-QP2010.

Table S1. Theoretical and experimental Wt% and At% values for EDS analysis on the MMFC composite.

Elements of MMFC	Wt% value		At% value	
	Theoretical	Experimental	Theoretical	Experimental
Mg	4.01	2.3	4.24	2.62
O	26.77	32.3	28.26	63.57
Fe	37.34	18.76	36.75	10.58
Cu	31.8	46.9	30.7	23.23

Table S2. The crystalline parameters for catalysts.

Samples	Space group	Lattice constant	Volume	Density	Site occupancy					Atom pair	Bond length	Bond Angel
CuO	C12/c1	a = 4.6890 b = 3.4253 c = 5.1320	81.28	6.50		x	y	z	occ	Cu-O	1.971	87.1
					Cu	0.25	0.25	0	1			
					O	0	0.3944	0.25	1			
MMF	C12/c1	a = 4.7743 b = 3.4283 c = 5.2057	83.72	6.31		x	y	z	occ	Cu-O	1.983	86.9
					Cu	0.25	0.25	0	1			
					O	0	0.4184	0.25	1			
	Fd-3m	a = 8.5280 b = 8.5280 c = 8.5280	620.20	5.09		x	y	z	Occ	Cu1/ Mg1/Fe1-O	2.060	90.3
					Cu1	0	0	0	0.25			
					Fe1	0	0	0	0.50			
					Mg1	0	0	0	0.25			
					Cu2	0.6250	0.6250	0.6250	0.25	Cu2/ Mg2/Fe2-O	1.890	88.7
					Fe2	0.6250	0.6250	0.6250	0.50			
					Mg2	0.6250	0.6250	0.6250	0.25			
					O	0.4038	0.4038	0.4038	1			
MMFC	C12/c1	a = 4.7270 b = 3.4052 c = 5.1040	81.02	6.52		x	y	z	occ	Cu-O	1.984	86.5
					Cu	0.25	0.25	0	1			
					O	0	0.4187	0.25	1			
	Fd-3m	a = 8.3810 b = 8.3810 c = 8.3810	588.7	4.82		x	y	z	Occ	Cu1/ Mg1/Fe1-O	2.087	89.6
					Cu1	0	0	0	0.25			
					Fe1	0	0	0	0.50			
					Mg1	0	0	0	0.25			
					Cu2	0.6250	0.6250	0.6250	0.25	Cu2/ Mg2/Fe2-O	1.901	88.2
					Fe2	0.6250	0.6250	0.6250	0.50			
					Mg2	0.6250	0.6250	0.6250	0.25			
					O	0.3976	0.3976	0.3976	1			

Table S3.

The textural characteristics of the as-fabricated catalysts.

Sample	$S_{BET}(m^2/g)$	$V_t^a(\ cm^3/g)$	$V_m^b(\ cm^3/g)$	$D_p^c(\ nm)$	Pore structure
CuO	12.8	0.138	2.94	43.36	Mesopore
MMF	0.366	0.0074	0.084	81.52	Macropore
MMFC	13.22	0. 064	3.038	19.52	Mesopore

Table S4.

The physicochemical properties of the water samples.

Physicochemical parameters	Unit	DI-W	TW	RW	LW	SWE
pH	--	7.44	7.36	7.8	8.2	7.5
Nitrate nitrogen	mg/L	0.004	0.22	0.37	4.35	9.46
Phosphate	mg/L	0.001	0.02	0.325	0.68	2.78
Chloride	mg/L	0.003	298.7	1243.7	2785.6	1436.5
Electrical conductivity	mS/cm	0.01	ND	0.56	1.47	0.87
TOC	mg/L	0.18	1.75	7.87	14.5	18.8
COD	mg/L	ND	1.04	18.6	25.85	44.65
Suspended solids (SS)	mg/L	ND	ND	2.55	3.84	9.65

Products	(m/z)	Molecular Formula	Proposed Structure	Retention Time (min)
CIP	332.13	$C_{17}H_{18}FN_3O_3$	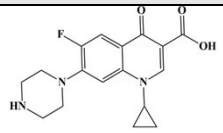	2.91

Table S5. Partial information on CIP and its analogs.

P1	334.11	$C_{16}H_{16}FN_3O_4$	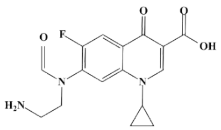	2.586
P2	350.08	$C_{17}H_{20}FN_3O_4$	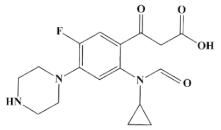	2.724
P3	334.11	$C_{16}H_{19}N_3O_5$	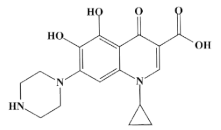	2.586
P4	263.08	$C_{13}H_{11}N_2O_3F$	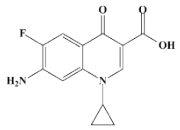	3.701
P5	237.08	$C_{11}H_{10}N_2O_4$	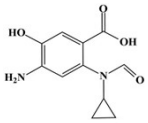	1.215
P6	283.09	$C_{12}H_{11}FN_2O_5$	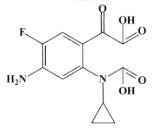	1.215
P7	285.07	$C_{16}H_{15}N_3O_2$	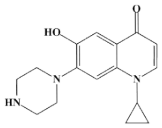	3.703
P8	184.02	$C_8H_6FNO_3$	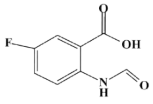	1.216

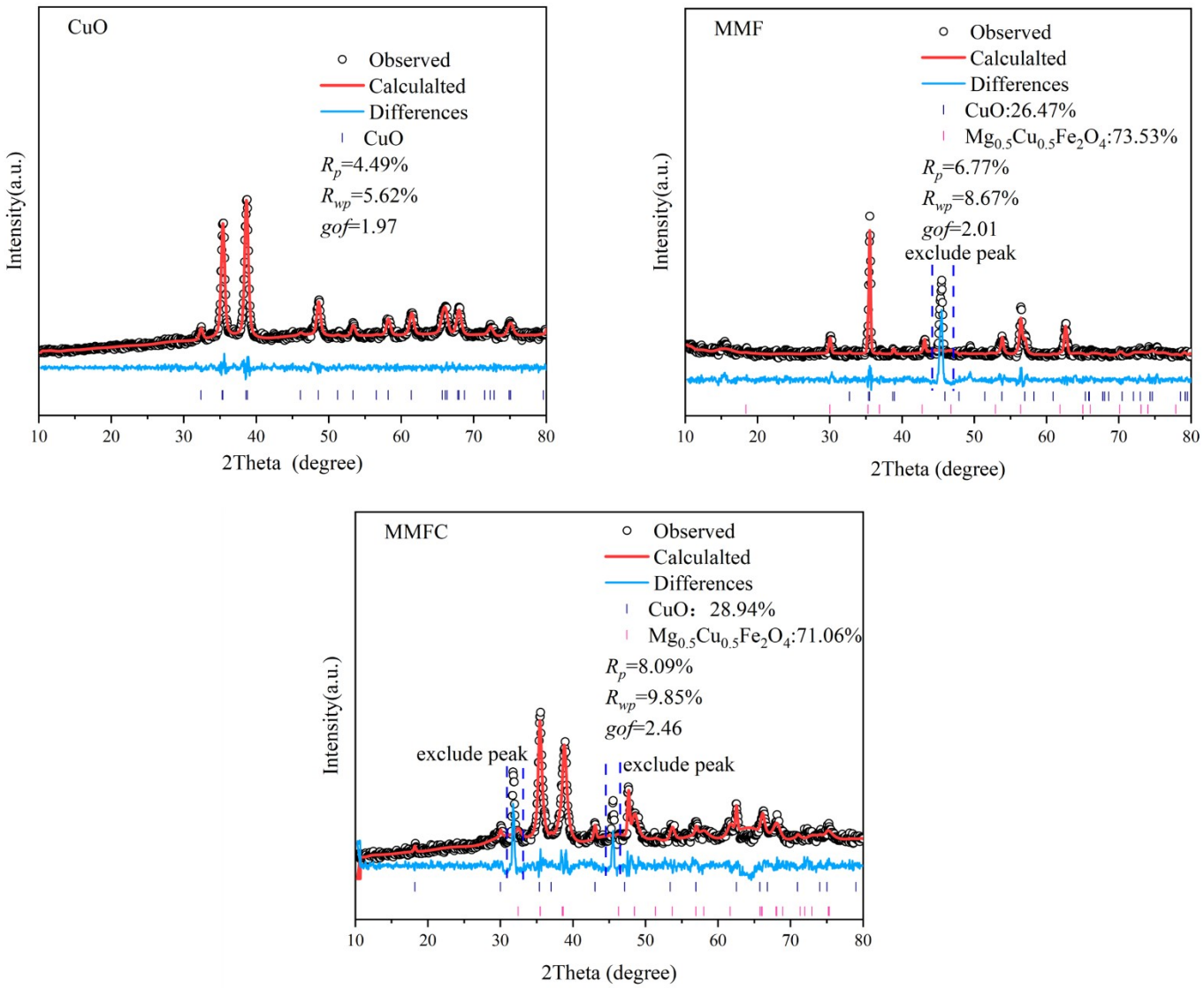

Fig. S1: XRD pattern refinements using the Rietveld method of CuO, MMF and MMFC.

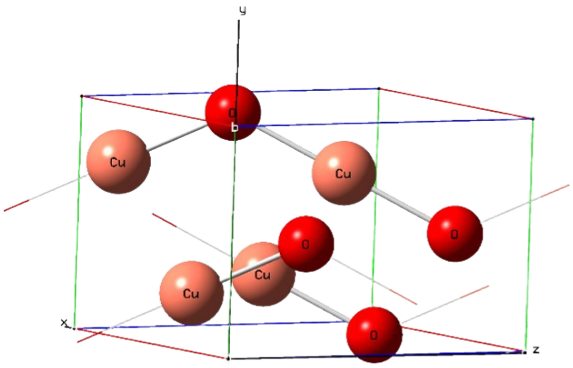

Fig. S2: The unit cell structure of CuO

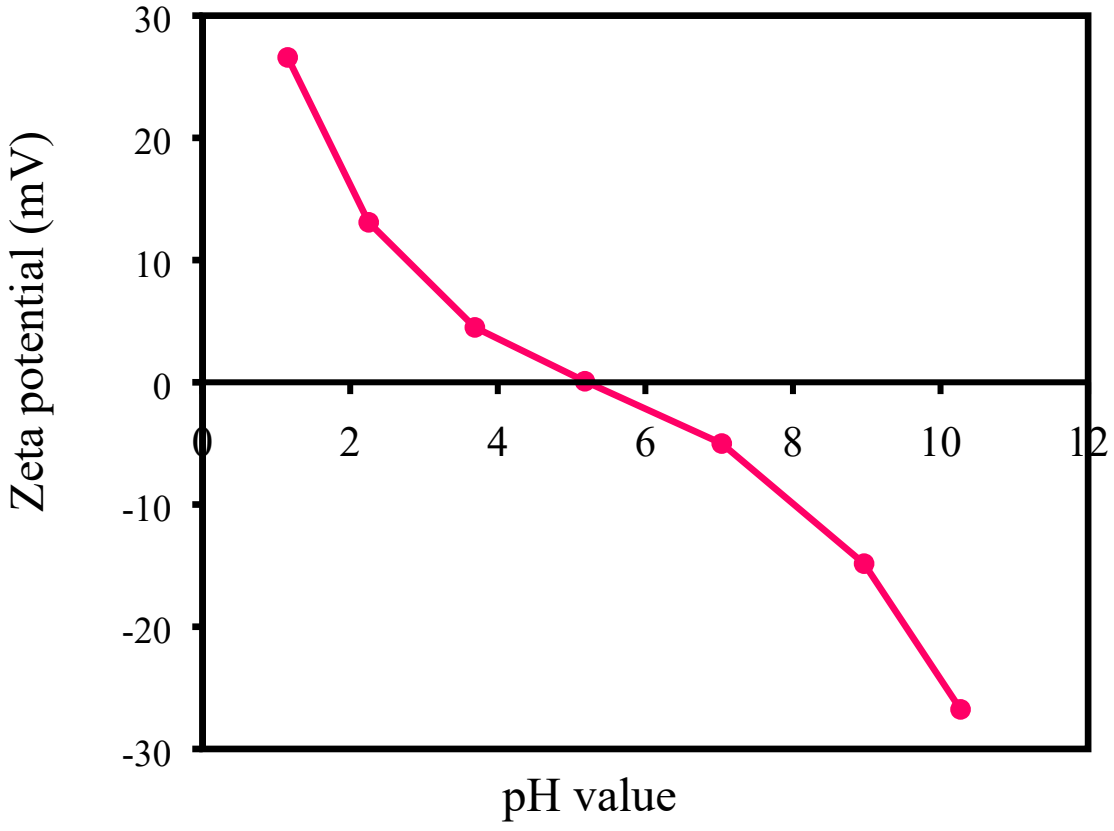

Fig. S3. Zeta potential of MMFC in the pH range of 1.0-11.0.

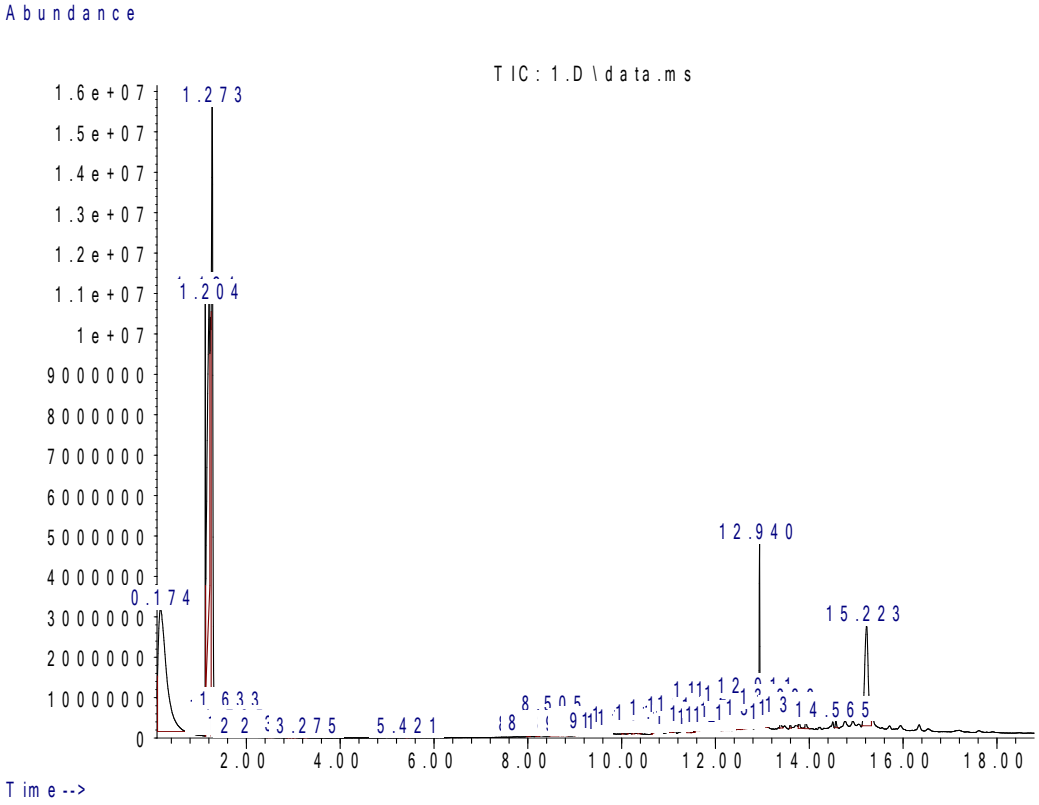

Fig. S4: MS spectra of CIP degradation intermediates obtained by the GC-MS method.